# Diffraction from quasicrystals: Geometric structure factor

Marko V. Jarić*
*Department of Physics, Harvard University, Cambridge, Massachusetts 02138*
(Received 23 January 1986)

A quasicrystal may be described by its quasilattice and its atomic decoration. We discuss two different commonly used methods for decorating quasilattices which lead to inequivalent real-space structures, the tile-decoration method and the hyperlattice-decoration-and-projection method. It is shown that diffraction patterns of such quasicrystals cannot be generally split into the intrinsic structure factor, due to the quasilattice, and the geometric structure factor, due to the decoration. For the hyperlattice decoration the zero-wave-vector limit cannot separate the quasilattice and the decoration contributions. However, such separation does occur for certain simple sequences of wave vectors and the tile-decorated quasilattices. We point to the ambiguities in choosing the "unit tiles" of a quasicrystal and we emphasize that the number of "atoms" per tile can be fractional. We have focused on two-dimensional pentagonal quasicrystals but some of our conclusions and results survive generalizations to other cases.

## I. INTRODUCTION

Significant activity was generated among condensed-matter theorists when the discovery of Bragg diffraction patterns with icosahedral symmetry was recently reported.[1] The discovery called for an explanation of the structure and the diffraction patterns of a new "quasicrystalline" phase of matter. Interestingly, several years earlier Mackay speculated about precisely such a phase[2] and he even published optical diffraction from a pentagonal quasicrystalline pattern.[3] Subsequently, several groups[4–10] were able, by using different but related methods,[11] to construct certain simple quasilattices[12] which generated required icosahedral diffraction patterns. These methods were based on a view of a quasilattice as a projection (or a section) of a portion of a simple higher dimensional periodic lattice (hyperlattice).[13,14] This approach was originally applied to ordinary incommensurate crystals by deWolff[15] and Janner and Janssen[16] who demonstrated, as emphasized clearly by Bak,[17] that a quasiperiodic structure can be *always* viewed as a *cut* through a higher-dimensional periodic structure.

Although it was immediately realized that quasicrystals of arbitrary symmetry could be constructed and analyzed,[9,18] most of the recent work inspired by Schechtman's discovery was focused on icosahedral quasilattices. It was first published by Mackay[2,3] that an icosahedral tiling (quasilattice) can be constructed using a pair of "unit cells."[19] The construction is specified in terms of division ("inflation") rules.[20,21] Later, Kramer and Neri[14] showed that an icosahedral quasilattice can be constructed as a projection from a six-dimensional simple hypercubic lattice. Subsequently, the diffraction patterns of icosahedral quasilattices were studied by many authors[4–10] and the diffraction from *simple* quasilattices seems essentially understood. It remains to investigate the effects of the quasilattice decoration on the diffraction patterns.

Immediately after the experimental discoveries it was shown that certain icosahedral quasilattices can be related to one-dimensional quasilattices represented by Fibonacci sequences of short and long intervals.[4] Ostlund and Pandit[22] were recently interested in the spectrum of an electron moving in a quasiperiodic potential somewhat similar to the potential which might be generated by the one-dimensional Fibonacci quasilattice.[23,24] Later, the Fibonacci quasilattice served as the favored pedagogical illustration of the projection method for constructing the quasilattices and their diffraction patterns.

Comparatively little attention has been paid to two-dimensional quasilattices. This is somewhat surprising since the two-dimensional quasilattices were intensely investigated in the context of nonperiodic tilings.[25] This study culminated in the discovery of pentagonal tilings by Penrose.[26] The Penrose quasilattice[27] was subsequently studied in great detail by deBruijn[13] who also showed how the Penrose quasilattice can be constructed as a projection from a five-dimensional simple hypercubic lattice. It was a generalization of the Penrose quasilattice that led to the construction of the three-dimensional icosahedral quasilattice.

The present paper is devoted to a detailed study of decagonal quasilattices and their diffraction patterns. We are mainly motivated by Bendersky's recent discovery of a new quasicrystalline phase of aluminum manganese, the so-called $T$ phase.[28] This phase, which appears to interpolate between an icosahedral phase and a crystalline phase, is characterized by simple periodicity in one direction and decagonal quasiperiodicity in the perpendicular planes. An understanding of the $T$ phase appears essential for illumination of quasiperiodicity in aluminum-manganese alloys. However, we shall not attempt to determine the actual structure of this phase in this paper. Here, we rather want to do the necessary ground work which is also sufficiently broad to survive future generalizations.

Our motivation is also pedagogical. Two-dimensional

 

quasilattices offer a nontrivial example of the projection technique and they illustrate certain complications which are absent from previously investigated one- and three-dimensional cases. Such complications may show up in cases of more general quasilattices.

Additionally, two-dimensional quasilattices can be used to illustrate the role played by the quasilattice decoration. Since the real quasicrystals are likely to correspond to decorated quasilattices this role must be elucidated.

In the following section we shall apply the projection method to construct two-dimensional decagonal quasilattices. This will essentially review the relevant parts of deBruijn's work. Then, we shall discuss the two commonly used ways of decorating (placing "atoms" in) the quasilattices. The first way is to decorate the associated hypercubic lattice and then project, while the second way is to directly decorate the "unit cells" (or, "tiles") of the quasilattice. We shall see that the two methods are *not* generally equivalent although the structures obtained by either method can be always represented as cuts through higher dimensional periodic structures. For the tiling-decoration method the specification of the shapes of the fundamental tiles is essential. This is in sharp contrast to ordinary crystals for which the ambiguity in defining the unit cells is superficial. Another difference from ordinary crystals will be in that a unit cell of a quasicrystal may contain a fractional number of atoms.

In the fourth section we shall calculate the scattering intensity (the structure factor) for decagonal quasilattices. Using the usual methods, we shall show that the diffraction pattern consists of sharp peaks which densely fill the entire space but whose amplitudes are rapidly varying functions of the scattering wave vector. This dependence of the amplitudes, which has no counterpart in crystals, will be characterized by an *intrinsic structure factor* which we shall explicitly calculate. Then, in the next section, we shall investigate the effect which decoration of the quasilattice has on the structure factor. The effect will be different for the two different ways of decorating the quasilattice. However, in either case, only under certain conditions will the effect of decoration be expressible in terms of a *geometric structure factor* analogously to the case of crystals. We shall particularly investigate the structure factor near the origin and we shall suggest some experimentally observable differences between the two methods of decorating the quasilattices.

In Appendix A we shall give some details of the geometry of nonsingular Penrose quasilattices. For one-, two-, and three-dimensional quasilattices, we shall derive in Appendix B certain sequences of wave vectors which are suitable for investigating zero- and infinite-wave-vector limits of the structure factor. In Appendix C we shall give geometric results necessary for calculating diffraction patterns of a general pentagonal quasilattice.

## II. PENTAGONAL QUASILATTICES

In 1974 Penrose[26] discovered a pair of tiles, kites, and darts, which, when combined with a specific matching rule can tile a plane only nonperiodically (see Fig. 1). The Penrose tiling has many fascinating properties: it has a

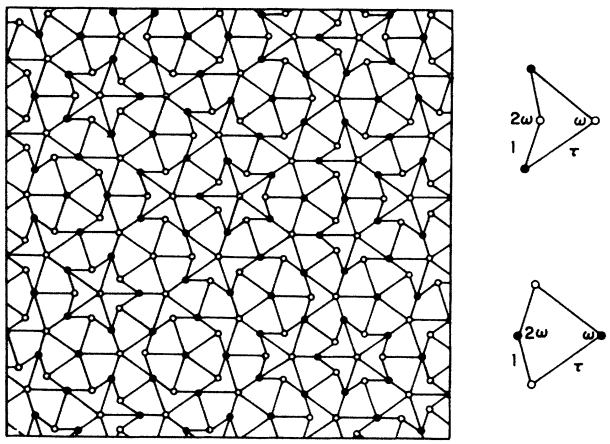


FIG. 1. Penrose tiling in terms of kites and darts. The matching rules are enforced by matching equal color vertices. [$\omega=2\pi/5$, $\tau=(1+\sqrt{5})/2$.]

macroscopic (average) tenfold symmetry, long-range decagonal bond-orientational symmetry, and many centers of local fivefold symmetry; the tiling is self-similar and can be constructed by an inflation procedure; the ratio of darts to kites is the golden mean $\tau=(1+\sqrt{5})/2 \approx 1.618\ldots$; every finite portion of any tiling can be found in any other tiling with frequency of the order of its reciprocal area, etc. We shall not attempt to review all the aspects of the Penrose tiling which can be found in a review by Gardner.[25] We shall only focus on these aspects which are most important to us.

An alternative pair of Penrose tiles, to which we shall later refer, are the two rhombuses, the "thick" and the "thin," shown in Fig. 2. The matching rule for these tiles is usually imposed by oriented edges of two colors. In Fig. 2 we also show a tiling with the thick and thin rhombuses. The vertices of a Penrose tiling form the Penrose quasilattice.

It will be useful for our future calculations to recall that eight different types of vertices occur in the Penrose tiling. They are identified in Fig. 3. These types of vertices are in one-to-one correspondence with the types of Voro-

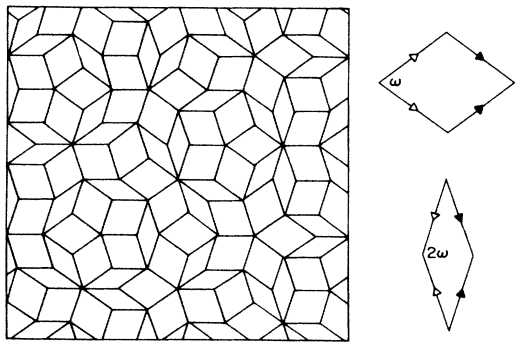


FIG. 2. Penrose tiling in terms of thick and thin rhombuses. The matching rules enforce the matching of equal color arrows.

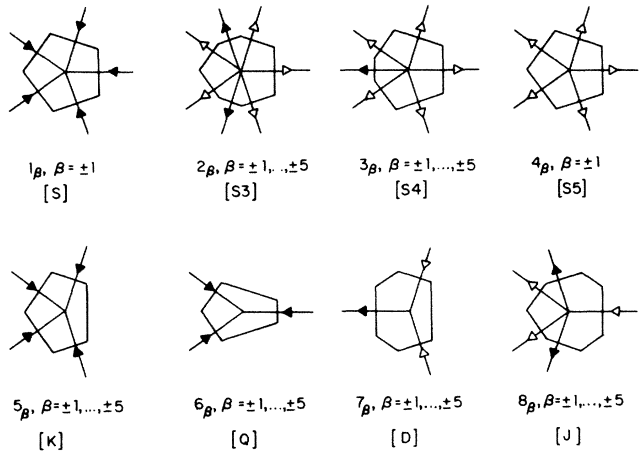


FIG. 3. Types of vertices and Voronoi polygons occurring in Penrose quasilattices. The vertices were identified in Ref. 13 whose notation we give in brackets. Our index $\mu\equiv\alpha_\beta$ identifies by $\alpha$ a particular type of vertex (polygon) while the subscript $\beta$ identifies its possible orientations relative to the orientation shown. For example, $\beta>0$ is associated with the rotation by $(\beta-1)\omega$, while $-\beta$ is the same rotation followed by a rotation by $\pi$.

noi polygons[29] associated with the quasilattice.[30] The frequency of occurrence of a Voronoi polygon as well as the fractional area occupied by its type of polygon are listed in Table I. They are calculated as explained in Appendix A. The vertices with fivefold symmetry have frequency $\approx 5.57\%$. We show in Fig. 4 the Penrose quasilattice and its tiling by the Voronoi polygons.[2] Vertices of the Voronoi polygons also specify a quasilattice with decagonal symmetry. However, this lattice can obviously be considered a decoration of the original Penrose quasilattice.

The construction of the Penrose quasilattice by the projection technique was first described by deBruijn.[13] The general method for constructing the quasilattices by projection is the following.

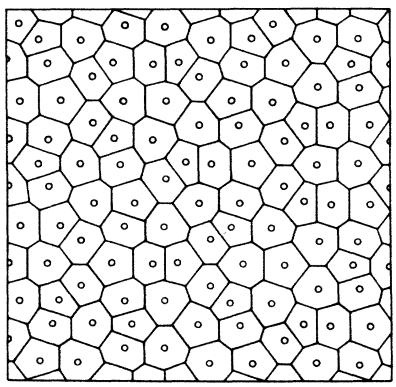

FIG. 4. Penrose quasilattice (vertices of Fig. 2) and its tiling by the Voronoi polygons shown in Fig. 3. See also Fig. 7 in Ref. 2.

Let $\mathbf{R}$ denote a lattice point of a $D$-dimensional periodic lattice.[31] Associated with the lattice is the density

$$\rho(\mathbf{x})=\sum_{\mathbf{R}}\delta(\mathbf{x}-\mathbf{R})\ . \tag{1}$$

Next, let us decompose the $D$-dimensional space into a $D^{\parallel}$-dimensional subspace and its orthogonal complement, $D^{\perp}$ dimensional subspace, $D=D^{\parallel}+D^{\perp}$. Then, choose a window function $W(\mathbf{x})$ which cuts from the lattice a slab "parallel" to the $D^{\parallel}$-dimensional subspace (see Fig. 5). The window function is usually a function of $\mathbf{x}^{\perp}$ only (note: $\mathbf{x}=\mathbf{x}^{\parallel}+\mathbf{x}^{\perp}$). Now, place the window at a point $\mathbf{y}$ and define a density in the parallel subspace by

$$\rho^{\parallel}(\mathbf{x}^{\parallel})=\int d\mathbf{x}^{\perp}\rho(\mathbf{x})W(\mathbf{x}-\mathbf{y})\ . \tag{2}$$

If $W(\mathbf{x})$ has a sharp cutoff,

$$W(\mathbf{x})=\begin{cases}1, & \mathbf{x}\in\Omega\\ 0, & \text{otherwise}\ ,\end{cases} \tag{3}$$

where $\Omega$ is the volume representing the window, then the density $\rho^{\parallel}$ consists of a set of $\delta$-functions of equal magnitude (except, perhaps, for the points at the boundary of the window). If the slab selected by the window has an "irrational" ("incommensurate") orientation this set specifies a quasilattice; for a rational orientation one would instead generate a lattice. Thus,

$$\rho^{\parallel}(\mathbf{x}^{\parallel})=\sum_{\mathbf{R}}\delta^{\parallel}(\mathbf{x}^{\parallel}-\mathbf{R}^{\parallel})W(\mathbf{R}-\mathbf{y})\ . \tag{4}$$

Although we started from density Eq. (1) we note that this density need not be a set of $\delta$ functions. Also the window function need not have a sharp cutoff.[32] However, since we are interested in quasilattices[12] when possible we shall interpret in this paper such variations as resulting from a *decoration* of a quasilattice.

The set of quasilattices obtained in this way (for a given choice of the window) can be parametrized by $\mathbf{y}$. Since different $\mathbf{y}^{\parallel}$ correspond to translations of the quasilattice, one can set $\mathbf{y}^{\parallel}=0$ without any loss of generality. The perpendicular component $\mathbf{y}^{\perp}$ can be obviously restricted to lay within the perpendicular projection $U^{\perp}$ of the unit cell $U$ of the hyperlattice (see Fig. 5).

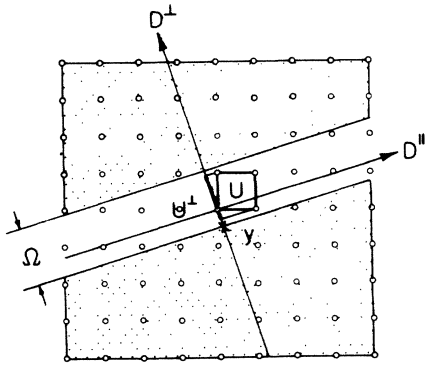


FIG. 5. Schematic representation of a slab (unshaded region) cut out of a periodic lattice. The points inside the slab are projected onto the || subspace to give a quasilattice. (See the text.)

TABLE I. Frequencies of the vertices in a regular Penrose tiling. The vertices are shown in Fig. 3 which also defines the indices given in the first column. Areas of the Voronoi tiles are given in third column while the areas in $\perp$ space shown in Fig. 7 are in column two (arbitrary units). Fourth and fifth columns give the frequency and the fractional area of the tiles.

| $\mu$ | $A_\mu^\perp$ | $A_\mu^\parallel$ | $p_\mu^\perp$ | $p_\mu^\parallel$ |
|---|---|---|---|---|
| $1_\beta$, $\beta=\pm1$ | $3\tau+1$ | $10\tau-5$ | $\frac{1}{10}(18-11\tau)\approx2.016\%$ | $\frac{1}{4}(5\tau-8)\approx2.254\%$ |
| $2_\beta$, $\beta=\pm1,\ldots,\pm5$ | $\tau$ | $6\tau+1$ | $\frac{1}{10}(13-8\tau)\approx0.557$ | $\frac{1}{100}(22\tau-35)\approx0.597$ |
| $3_\beta$, $\beta=\pm1,\ldots,\pm5$ | 1 | $8\tau-2$ | $\frac{1}{10}(13\tau-21)\approx0.344$ | $\frac{1}{50}(73-45\tau)\approx0.377$ |
| $4_\beta$, $\beta=\pm1$ | $2\tau-1$ | $10\tau-5$ | $\frac{1}{10}(47-29\tau)\approx0.770$ | $\frac{1}{4}(13\tau-21)\approx0.861$ |
| $5_\beta$, $\beta=\pm1,\ldots,\pm5$ | $\tau+1$ | $7\tau-2$ | $\frac{1}{10}(5\tau-8)\approx0.902$ | $\frac{1}{100}(51-31\tau)\approx0.841$ |
| $6_\beta$, $\beta=\pm1,\ldots,\pm5$ | $2\tau+1$ | $4\tau+1$ | $\frac{1}{10}(5-3\tau)\approx1.459$ | $\frac{1}{100}(5\tau-7)\approx1.090$ |
| $7_\beta$, $\beta=\pm1,\ldots,\pm5$ | $5\tau+3$ | $3\tau+5$ | $\frac{1}{10}(2-\tau)\approx3.820$ | $\frac{1}{100}(7-2\tau)\approx3.764$ |
| $8_\beta$, $\beta=\pm1,\ldots,\pm5$ | $3\tau+2$ | $4\tau+5$ | $\frac{1}{10}(2\tau-3)\approx2.361$ | $\frac{1}{100}(6\tau-7)\approx2.708$ |

We can now explicitly construct the pentagonal quasilattices which, following deBruijn, can be viewed as projections from a five-dimensional hypercubic lattice. Let us denote the orthonormal unit vectors generating the hyperlattice by[33] $\hat{\mathbf{e}}_j$, $j=1,\ldots,5$, where

$$\hat{\mathbf{e}}_j\cdot\hat{\mathbf{e}}_k=\delta_{jk}\ . \tag{5}$$

The fivefold symmetry in this case corresponds to cyclic permutations of $\hat{\mathbf{e}}_j$'s and its axis is the (1,1,1,1,1) axis. With respect to this symmetry, the five-dimensional space splits into three invariant subspaces: the two-dimensional subspace spanned by the unit vectors

$$\hat{\mathbf{a}}_1^\parallel=\sqrt{2/5}\,\mathrm{Re}(1,z,z^2,z^3,z^4) \tag{6}$$

and

$$\hat{\mathbf{a}}_2^\parallel=\sqrt{2/5}\,\mathrm{Im}(1,z,z^2,z^3,z^4)\ , \tag{7}$$

another two-dimensional subspace spanned by

$$\hat{\mathbf{a}}_1^\perp\equiv\hat{\mathbf{a}}_1^\perp=\sqrt{2/5}\,\mathrm{Re}(1,z^2,z^4,z,z^3) \tag{8}$$

and

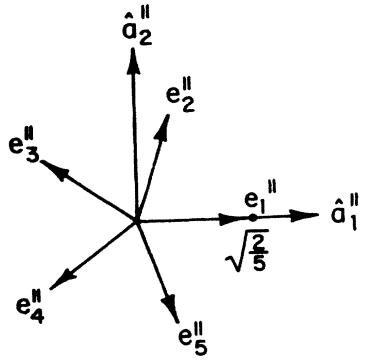


FIG. 6. Projections of the unit vectors $\hat{\mathbf{e}}_j$ of the hyperlattice into $\parallel$ subspace. The relative orientation of the **e**, and **a** vectore is, of course arbitrary. The orientation in the figure is the same as in Eqs. (6) and (7).

$$\hat{\mathbf{a}}_2^\perp\equiv\hat{\mathbf{a}}_2^\perp=\sqrt{2/5}\,\mathrm{Im}(1,z^2,z^4,z,z^3)\ ; \tag{9}$$

and a one-dimensional subspace spanned by

$$\hat{\mathbf{a}}_0^\perp=\frac{1}{\sqrt{5}}(1,1,1,1,1)\ , \tag{10}$$

where

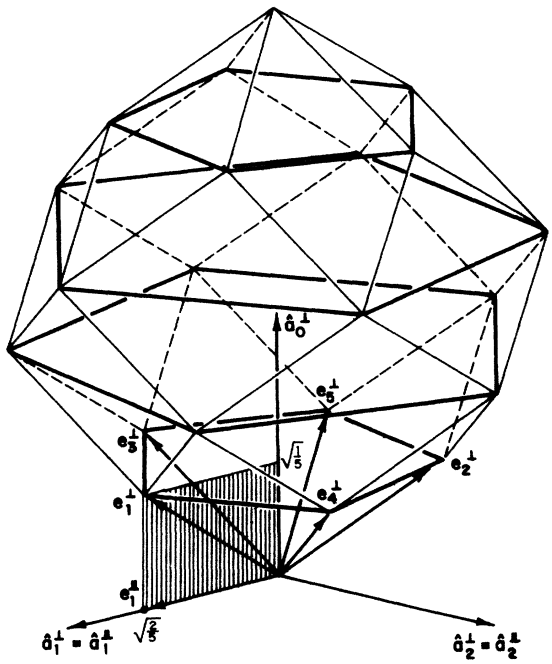


FIG. 7. Projections of the unit vectors $\hat{\mathbf{e}}_j$ of the hyperlattice into $\perp$ subspace. The orientations between the projections and the basis $\hat{\mathbf{a}}_j$ of the space are given by Eqs. (8) to (10). We also show the projection $U^\perp$ of the hypercubic unit cell as the interior of the rhombic icosahedron. Pentagonal sections of the icosahedron by the plans $x_0^\perp=M/\sqrt{5}$, $M=1,2,3,4$, are emphasized in the figure. For clarity, we do not show all $\mathbf{e}_j^\perp$; only $\mathbf{e}_1^\perp$ is given.

$$z \equiv \exp(i\omega) \tag{11}$$

and $\omega = 2\pi/5$. The components of the vectors $\hat{\mathbf{e}}_j$ in the $||$ and $\perp$ subspaces are shown in Figs. 6 and 7, respectively. Algebraically, they are given by

$$\mathbf{e}_j^{||} = P^{||}\hat{\mathbf{e}}_j \tag{12}$$

and

$$\mathbf{e}_j^{\perp} = P^{\perp}\hat{\mathbf{e}}_j = (1 - P^{||})\hat{\mathbf{e}}_j \ , \tag{13}$$

where the projector $P^{||}$ is

$$P_{jk}^{||} = \sum_{l=1}^{2} (\hat{\mathbf{a}}_l^{||} \cdot \hat{\mathbf{e}}_j)(\hat{\mathbf{a}}_l^{||} \cdot \hat{\mathbf{e}}_k) = \tfrac{2}{5}\cos[(j-k)\omega] \ . \tag{14}$$

The window function which leads to the Penrose quasilattice is independent of $\mathbf{x}^{||}$,

$$W(\mathbf{x}) \equiv W(\mathbf{x}^{\perp}) = \begin{cases} 1, & \text{if } \mathbf{x}^{\perp} \in P^{\perp}U \equiv U^{\perp} \ , \\ 0, & \text{otherwise} \ , \end{cases} \tag{15}$$

where $U$ is the hyperlattice unit cell with a vertex at the origin and a vertex at (1,1,1,1,1). In Fig. 7 we also show $U^{\perp}$ as the interior of a rhombic icosahedron. Therefore, the quasilattice density is explicitly

$$\rho^{||}(\mathbf{x}^{||}) = \sum_{n_1=-\infty}^{\infty} \cdots \sum_{n_5=-\infty}^{\infty} \delta^{||}(\mathbf{x}^{||} - \Sigma n_j \mathbf{e}_j^{||}) \times W(\Sigma n_j \mathbf{e}_j^{\perp} - \mathbf{y}^{\perp}) \ . \tag{16}$$

As mentioned earlier, the parameter $\mathbf{y}$ can be restricted to $\mathbf{y}^{||} = 0$, that is,

$$y_1 + (y_2 + y_5)\cos\omega + (y_3 + y_4)\cos(2\omega) = 0 \ , \tag{17}$$

and

$$(y_2 - y_5)\sin\omega + (y_3 - y_4)\sin(2\omega) = 0 \ . \tag{18}$$

Therefore, we are left with a three-parameter family,

$$\mathbf{y} = \mathbf{y}^{\perp} \in U^{\perp} \tag{19}$$

of possible pentagonal quasilattices.[34]

It was pointed out by deBruijn[13] that the Penrose quasilattices correspond to $y_0^{\perp} = 0$, that is,

$$y_1 + y_2 + y_3 + y_4 + y_5 = 0 \ . \tag{20}$$

Equations (17) through (20) specify a two-dimensional family of Penrose quasilattices which are labeled by

$$\mathbf{y} = \mathbf{y}^{\perp\perp} \in U^{\perp\perp} \ . \tag{21}$$

DeBruijn also showed that this family can be further split into the ordinary, or *regular,* Penrose quasilattices and the *singular* and the *exceptionally singular* Penrose quasilattices.[35] The singular Penrose quasilattices are labeled by $\mathbf{y}$ which in addition to satisfying (21) also satisfies

$$\mathbf{y}^{\perp} = b(\mathbf{e}_l^{\perp} - \mathbf{e}_k^{\perp}) + \sum_{j=1}^{5} m_j \mathbf{e}_j^{\perp} \tag{22}$$

for some $l \neq k$, some real $b$, and some integers $m_j$. Note that (20) implies $\sum_{j=1}^{5} m_j = 0$. If, in addition, $b = 0$ then the quasilattice is called *exceptionally singular.*

The exceptionally singular Penrose quasilattices have an exact $C_{10v}$ symmetry and the corresponding $\mathbf{y}$ is such that the $||$ subspace, when shifted to $\mathbf{y}$, will *contain* a lattice point. Precisely this point becomes the center of the symmetry. Similarly, a singular Penrose quasilattice has an exact mirror symmetry. We display in Fig. 8 typical regular and singular Penrose quasilattices and we also show the extended Penrose quasilattices associated with $y_0^{\perp} \neq 0$. We see that the main differences are in the exact symmetry of the quasilattice, in some local variation of the density of lattice points,[36] and in the types and frequencies of vertices. Note, however, that in all cases the average density of vertices is the same

$$\overline{\rho^{||}} = \lim_{V^{||} \to \infty} \frac{1}{V^{||}} \int_{V^{||}} \rho^{||}(\mathbf{x}^{||}) d\mathbf{x}^{||} = \frac{V^{\perp}(U^{\perp})}{V(U)} = (2+\tau)/5 \approx 0.7236 \ldots , \tag{23}$$

in units of vertex/area of thin rhombus.

In the following sections we shall also see that all types of Penrose quasilattices lead to the same qualitative features of the diffraction pattern. That is, they all give rise to Bragg peaks at the identical positions. However, relative intensities of the peaks although independent of $\mathbf{y}^{||}$ will generally depend on $y_0^{\perp}$.

## III. PENTAGONAL QUASICRYSTALS

Just as in the case of ordinary crystals, a specification of a quasicrystalline structure requires more than the knowledge of its (quasi)lattice. Given a crystal lattice one needs to describe the atomic content, or *decoration,* of the unit cell, the unit cell being specified by a tiling associated with the lattice. Precisely analogous procedure can be used to specify structure of a quasicrystal.[37,38] One can first specify a tiling associated with the quasilattice, e.g., the Penrose tiling of the Penrose quasilattice, and then one can specify a decoration of the different *unit tiles.* For example, the two Penrose rhombuses can be given a decoration. The only requirement on the decoration is that it respects the matching rules. However, unlike the ordinary crystals, a Penrose tile can be found in several different local environments and one would expect that in a "real quasicrystal" the atoms would relax into new positions according to the different local environment they see. This would, in turn, lead to a new varying, decorations of the same tile. It might be, therefore, more reasonable to consider a quasicrystal as a projection of a hypercrystal, that is, to decorate the hypercubic lattice and then make the projection. The decorations of the quasilattices obtained in this way are not in general equivalent to any particular decoration of a *finite* number of unit tiles. Since the two procedures of decorating a quasilattice lead to differences in the diffraction patterns (as will be seen in Sec. V) we shall describe both of them.

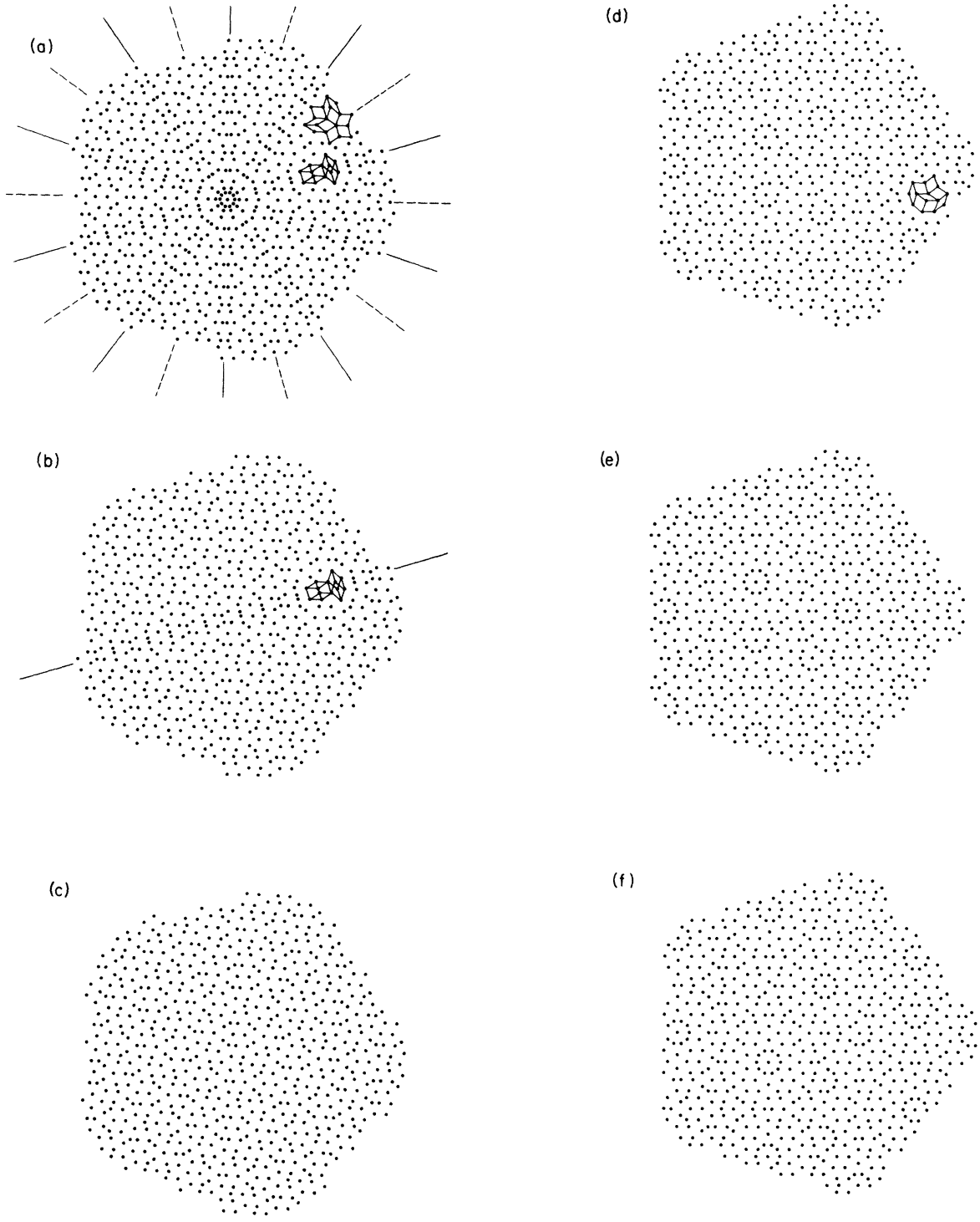


FIG. 8. Penrose and extended Penrose quasilattices. (a) The exceptionally singular Penrose quasilattice with $\mathbf{y}=0$. Clearly, the lattice has $C_{10v}$ symmetry with the mirror planes indicated in the figure. We show also portions of regular Penrose tiling and the portions with increased local density due to scrambling of the tiles. This scrambling violates the matching rules. By moving $\mathbf{y}$ inside the $\mathbf{y}_0^{\perp}=0$ plane the tiling can be unscrambled leaving only a mirror symmetry, as for the singular tiling in (b) where $\mathbf{y}=(0.0533,-0.0533,0,0,0)$, or no symmetry at all, as for the regular tiling in (c) where $\mathbf{y}=(0.0111,0.0123,0.0211,-0.0200,-0.0245)$. In (d), (e), and (f) we show the tilings resulting by shifting $\mathbf{y}$ of corresponding tilings in (a), (b), and (c) by $\mathbf{y}_0=\mathbf{a}_0^{\perp}/2\sqrt{5}=1/10(1,1,1,1,1)$. These tilings contain local arrangements of the tiles which would violate the matching rules for the Penrose tiles given in Fig. 2. Such examples are indicated in the figure. Note, however, that such tile combinations do occur in the sections of the three-dimensional icosahedral tilings. The reader is encouraged to copy the tiles on transparencies and to compare them. In particular, the reader can verify that tilings in (e) and (f) do not have exact pentagonal symmetry; the center of the tilings is only a local fivefold center.

The decoration of the hyperlattice can be described by the density

$$\rho(\mathbf{x})=\sum_{\mathbf{R}}\sum_{\xi} f_{\xi}\delta(\mathbf{x}-\mathbf{R}-\xi)\ , \tag{24}$$

where $\xi$ is the position of the $\xi$th atom in the hyperunit cell and $f_{\xi}$ is its scattering amplitude. The associated decoration of the quasilattice is in this case simply described by

$$\rho^{\parallel}(\mathbf{x}^{\parallel})=\sum_{\mathbf{R}}\sum_{\xi} f_{\xi}\delta^{\parallel}(\mathbf{x}^{\parallel}-\mathbf{R}^{\parallel}-\xi^{\parallel})W(\mathbf{R}+\xi-\mathbf{y})\ . \tag{25}$$

This follows immediately from Eqs. (2) and (24). In this expression there are no conditions on $\xi$'s except that in order to remove redundancy no two different $\xi$'s should have identical parallel components.

A direct decoration of a quasilattice can be accomplished by constructing at each quasilattice point a Voronoi polygon as described in Sec. II. These polygons can be taken as the unit tiles associated with the quasilattice. Generally, as in periodic lattices, only a finite number of distinct polygons will be generated. For example, it was mentioned earlier and it is shown in Appendix A that eight Voronoi polygons appear in regular Penrose quasilattices (see Fig. 3). However, in contrast to periodic lattices, every Voronoi polygon will be found in infinitely many distinct, infinite environments.

It is reasonable to decorate all identical Voronoi tiles in identical fashion. This should be a good approximation (to lowest order) since the shape of a Voronoi tile is completely determined by the immediate surrounding of its quasilattice point. Corrections may be obtained by distinguishing the tiles according to further neighbor environments. The decoration of the tiles should preserve their local symmetries and it must be consistent with the matching of the tiles. This matching condition leads to an interesting aspect of quasicrystals, namely, the number of atoms per unit tile need not be integral. For example, the number of atoms per thick or thin Penrose rhombus, if they are taken as unit tiles, must be an integer $\pm\frac{1}{5}$ or $\pm\frac{2}{5}$, respectively.

The resulting density for such decoration of unit tiles can be expressed as

$$\rho^{\parallel}(\mathbf{x}^{\parallel})=\sum_{\mu}\sum_{\mathbf{R}_{\mu}^{\parallel}}\sum_{\xi_{\mu}^{\parallel}} f_{\mu\xi_{\mu}^{\parallel}}\delta^{\parallel}(\mathbf{x}^{\parallel}-\mathbf{R}_{\mu}^{\parallel}-\xi_{\mu}^{\parallel})\ , \tag{26}$$

where $\mu$ indexes different (Voronoi) tiles and $\xi_{\mu}^{\parallel}$ is the position of $\xi_{\mu}^{\parallel}$th atom inside the $\mu$th tile (which is centered at the quasilattice point $\mathbf{R}_{\mu}^{\parallel}$). The corresponding atomic scattering amplitude is $f_{\mu\xi_{\mu}^{\parallel}}$. Generally, one will be able to define disjoint window functions $W_{\mu}(\mathbf{x})$ for each type of tiles (see Appendix A). That is

$$W_{\mu}(\mathbf{x})=\begin{cases}1, & \mathbf{x}\in\Omega_{\mu}\\ 0, & \text{otherwise}\end{cases}\ , \tag{27}$$

where

$$W(\mathbf{x})=\sum_{\mu} W_{\mu}(\mathbf{x})\ ,$$

$$\Omega=\bigcup\nolimits_{\mu}\Omega_{\mu}\ ,$$

and

$$\Omega_{\mu}\bigcap\Omega_{\nu}=\varnothing\ .$$

Hence, Eq. (26) can be rewritten as

$$\rho^{\parallel}(\mathbf{x}^{\parallel})=\sum_{\mu}\sum_{\mathbf{R}}\sum_{\xi_{\mu}} f_{\mu\xi_{\mu}}\delta^{\parallel}(\mathbf{x}^{\parallel}-\mathbf{R}^{\parallel}-\xi_{\mu}^{\parallel})W_{\mu}(\mathbf{R}-\mathbf{y})\ . \tag{28}$$

For example, in case of Penrose tiles $\mathbf{R}^{\perp}$ densely fills equidistant planes separated by $1/\sqrt{5}$ and perpendicular to the $\hat{\mathbf{a}}_0^{\perp}$ axis. The Penrose window $\Omega=U$ cuts four of these planes into pentagonal regions shown in Fig. 7. The intersections of these planes with the windows $\Omega_{\mu}=U_{\mu}$ corresponding to different Voronoi polygons have been also determined by deBruijn[13] and they are shown in Fig. 9. They are all filled with equal, uniform density of $\mathbf{R}_{\mu}^{\perp}$'s. This last fact is useful for calculating frequency of various subpatterns of Penrose quasilattices[39] and, in particular, for the frequency and fractional area of different Voronoi tiles calculated in Appendix A.

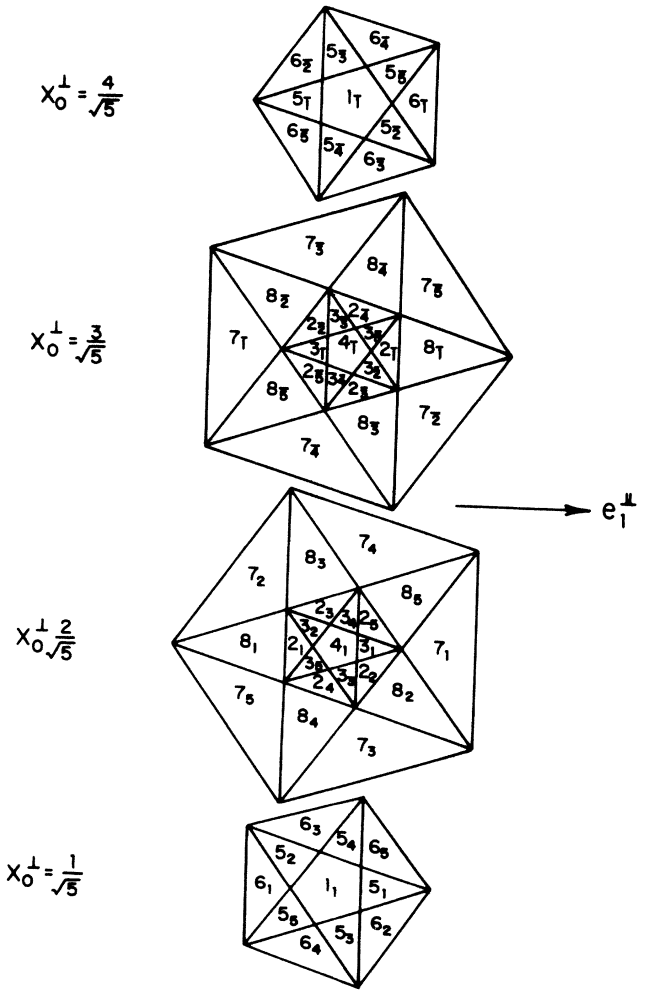


FIG. 9. Division of the pentagonal regions from Fig. 7 according to the different types of Voronoi polygons shown in Fig. 3. Note that the bar over a number indicates the negative number. Also note that the symbols $K$ and $Q$ should be exchanged in Fig. 8 of Ref. 13.

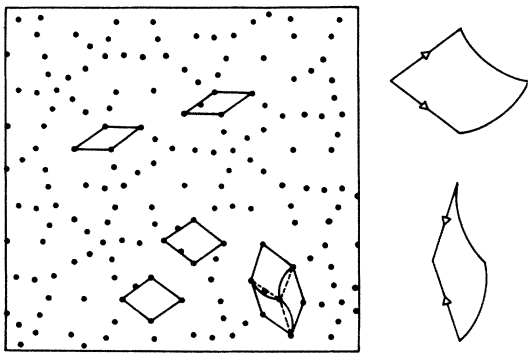

FIG. 10. A decoration of the Penrose quasilattice of Fig. 2 which *cannot* be expressed as a decoration of the two rhombuses. The decoration is achieved using *identically* decorated tiles shown at the right and around a vertex of the quasilattice. We also indicate pairs of identical rhombuses which, in contrast, appear with different decorations.

An alternative to decorating the Voronoi tiling of the quasilattice is to decorate its dual tiling. In general, the two decorations are not equivalent. For Penrose quasilattices, it turns out that the decoration of the quasilattice is more general. Moreover, for Penrose quasilattices one could also decorate either the rhombuses or the kites and the darts. Again, the latter decoration would be less general. However, this "arbitrariness" indicates possible difficulties which may arise in more general quasilattices. For example, any given tiling can be congruently deformed to another tiling. Such congruent deformations of the unit cell of a periodic lattice are inconsequential. In contrast, decoration of quasicrystalline unit tiles is, generally, not equivalent to a decoration of congruently deformed unit tiles. For Penrose quasilattices we illustrate this in Fig. 10. Clearly, then, to decorate a quasilattice one has to consider the *shapes* of the tiles as well as their decoration.

## IV. INTRINSIC STRUCTURE FACTOR

The scattering intensity from a density $\rho(\mathbf{x})$ of scatterers is proportional to the square of the Fourier transform of the density,

$$S(\mathbf{q}) \sim |\rho(\mathbf{q})|^2 , \tag{29}$$

where $\mathbf{q}$ is the scattering wave vector. For a crystal, $S$ splits into two factors,

$$S(\mathbf{q}) \sim I(\mathbf{q}) G(\mathbf{q}) . \tag{30}$$

The first factor leads to identical Bragg peaks located at the reciprocal lattice vectors. This factor we may call the *intrinsic* structure factor since it is independent of the specific decoration of the lattice. We shall see that for quasilattices the intrinsic structure factor is much richer.

The second factor is the *geometric* structure factor. It accounts for the scattering from the atoms within a single unit cell, that is,

$$G(\mathbf{q}) \sim \left| \sum_{\xi} e^{2\pi i \mathbf{q}\cdot\boldsymbol{\xi}} \right|^2 , \tag{31}$$

where $\xi$ is the position of the $\xi$th atom within a unit cell. In the next section we shall see that for quasicrystals a decomposition like in Eq. (30) is not always possible and we shall see to which extent it can be generalized. In the remainder of this section we shall discuss only the intrinsic structure factor of quasilattices.

The Fourier transform of Eq. (4) is

$$\rho^{\parallel}(\mathbf{q}^{\parallel}) = \int d\mathbf{q}^{\perp} e^{-2\pi i \mathbf{q}^{\perp}\cdot\mathbf{y}^{\perp}} \rho(\mathbf{q}) W^*(q^{\perp}) \sim \sum_{Q} \delta^{\parallel}(\mathbf{q}^{\parallel} - \mathbf{Q}^{\parallel}) W^*(\mathbf{Q}^{\perp}) e^{-2\pi i \mathbf{Q}^{\perp}\cdot\mathbf{y}^{\perp}} , \tag{32}$$

where $\mathbf{Q}$ is a reciprocal hyperlattice vector and we assumed that the window function depends only on $\mathbf{x}^{\perp}$. Therefore, the intrinsic structure factor leads to the sharp Bragg peaks at $\mathbf{q}^{\parallel} = \mathbf{Q}^{\parallel}$ whose intensity is

$$I(\mathbf{Q}^{\parallel}) \sim \left| \sum_{\mathbf{Q}=\mathbf{Q}^{\parallel}+\mathbf{Q}^{\perp}} e^{2\pi i Q^{\perp}\cdot\mathbf{y}^{\perp}} W(\mathbf{Q}^{\perp}) \right|^2 . \tag{33}$$

Unlike ordinary crystals, this set of Bragg peaks is dense in the whole plane. That is, every neighborhood of each point in the plane contains a peak. However, the peaks are isolated in the sense that sufficiently close to a given peak all other peaks are arbitrarily weak. The reason for this is that for two close $\mathbf{Q}^{\parallel}$'s corresponding $\mathbf{Q}^{\perp}$'s, which determine the intensities, are far apart.

For the one-dimensional Fibonacci quasilattices and the three-dimensional icosahedral quasilattices there is a one-to-one correspondence between the $\mathbf{Q}^{\parallel}$ and $\mathbf{Q}^{\perp}$ components of a reciprocal hyperlattice vector $\mathbf{Q}$. However, for Penrose quasilattices this correspondence is many to one. In fact, infinitely many different $\mathbf{Q}$'s have exactly the same $\mathbf{Q}^{\parallel}$ component. Explicitly, we write

$$\mathbf{Q} = (n_1, n_2, n_3, n_4, n_5) , \tag{34}$$

where $n_j$, $j = 1, \ldots, 5$ are integers. Then, according to Eqs. (6) to (10)

$$\mathbf{Q}^{\parallel} = \sqrt{2/5} \sum_j n_j (\cos[(j-1)\omega], \sin[(j-1)\omega]) , \tag{35}$$

$$\mathbf{Q}^{\perp\!\!\!\perp} = \sqrt{2/5} \sum_j n_j (\cos[2(j-1)\omega], \sin[2(j-1)\omega]) , \tag{36}$$

and

$$Q_0^{\perp} = \frac{1}{\sqrt{5}} \sum_j n_j , \tag{37}$$

where we expressed $\mathbf{Q}^{\parallel}$, $\mathbf{Q}^{\perp\!\!\!\perp}$, and $Q_0^{\perp}$ in the basis $(\hat{\mathbf{a}}_1^{\parallel}, \hat{\mathbf{a}}_2^{\parallel})$, $(\hat{\mathbf{a}}_1^{\perp\!\!\!\perp}, \hat{\mathbf{a}}_2^{\perp\!\!\!\perp})$, and $\hat{\mathbf{a}}_0^{\perp}$, respectively. Clearly, if every $n_j$ is replaced by $n_j + N$, where $N$ is an arbitrary integer, $\mathbf{Q}^{\parallel}$ and $\mathbf{Q}^{\perp\!\!\!\perp}$ remain unchanged while $Q_0^{\perp}$ increases by $N\sqrt{5}$. Therefore, although the correspondence between $\mathbf{Q}^{\parallel}$ and $\mathbf{Q}^{\perp}$ is one to infinity, the correspondence between $\mathbf{Q}^{\parallel}$ and $\mathbf{Q}^{\perp\!\!\!\perp}$ is one to one and Eq. (33) reduces to

$$I(\mathbf{Q}^{\parallel}) \sim \left| \sum_{N=-\infty}^{\infty} e^{2\pi i N y_0^{\perp} \sqrt{5}} W(\mathbf{Q}^{\perp\!\!\!\perp}, Q_0^{\perp} + N\sqrt{5}) \right|^2 . \tag{38}$$

Clearly, $Q_0^{\perp}\sqrt{5}=\sum_j n_j$ need only be specified mod5.

The infinite sum in Eq. (38) can be removed by going back to the direct space in the $\perp_0$ variables in which case Eq. (38) can be reduced to

$$I(\mathbf{Q}^{\parallel})\sim\left|\sum_{M=1}^{5} e^{i\omega M\sum n_j} W\left[\mathbf{Q}^{\perp\!\!\!\perp},\frac{M-\{y_0^{\perp}\sqrt{5}\}}{\sqrt{5}}\right]\right|^2, \quad (39)$$

where $\{x\}$ is the fractional part of $x$, $0\le\{x\}<1$. For regular and singular Penrose quasilattices $y_0^{\perp}=0$ and the intrinsic structure factor, which is independent of $\mathbf{y}^{\perp\!\!\!\perp}$, becomes identical for all Penrose quasilattices. Therefore, a scattering experiment could not distinguish between the regular and singular Penrose quasilattices. In fact, it could not distinguish the extended Penrose quasilattices with integer values of $y_0^{\perp}\sqrt{5}$. Generally, the intrinsic structure factor depends only on $\{y_0^{\perp}\sqrt{5}\}$, that is, on the intersection between the window $U$ and the planes $x_0^{\perp}=(M-\{y_0^{\perp}\sqrt{5}\})/\sqrt{5}$, $M=1,2,\ldots,5$. Consequently, although the real pentagonal quasilattices may be quite different for different $\mathbf{y}^{\perp\!\!\!\perp}$ and $y_0^{\perp}$ (see Fig. 8), and for fixed $\mathbf{y}^{\perp\!\!\!\perp}$ they depend on $\{y_0^{\perp}/\sqrt{5}\}$, the scattering intensity can only determine $\{y_0^{\perp}\sqrt{5}\}$ (see Fig. 11).[40]

Since the expression (38), from which Eq. (39) follows, contains a sum of terms, it is essential that relative phases of the individual terms are correct. Hence, Eq. (39) can be checked by evaluating directly the $\mathbf{Q}^{\parallel}$ Fourier transform of $\rho^{\parallel}(\mathbf{x}^{\parallel})$ [see Eq. (4)]. This gives

$$\rho^{\parallel}(\mathbf{Q}^{\parallel})=\sum_{\mathbf{R}} e^{2\pi i\mathbf{Q}^{\parallel}\cdot\mathbf{R}^{\parallel}} W(\mathbf{R}^{\perp}-\mathbf{y}^{\perp})$$
$$=\sum_{\mathbf{R}} e^{-2\pi i\mathbf{Q}^{\perp}\cdot\mathbf{R}^{\perp}} W(\mathbf{R}^{\perp}-\mathbf{y}^{\perp}), \quad (40)$$

where $\mathbf{Q}^{\perp}$ is the component of *any* reciprocal hyperlattice vector $\mathbf{Q}$ whose parallel component is $\mathbf{Q}^{\parallel}$. As mentioned above, $\mathbf{Q}^{\perp\!\!\!\perp}$ is unique while $Q_0^{\perp}$ is specified mod$\sqrt{5}$. The last sum in Eq. (40) can be split into a sum over $\mathbf{R}^{\perp\!\!\!\perp}$ and a sum over $R_0^{\perp}=M/\sqrt{5}$. However, we already mentioned that ponts $\mathbf{R}^{\perp\!\!\!\perp}$ are uniformly dense so their sum can be replaced by an integral[41] resulting in

$$I(\mathbf{Q}^{\parallel})\sim\left|\sum_{M=-\infty}^{\infty} e^{-i\omega M\sum n_j}\int d\mathbf{x}^{\perp\!\!\!\perp} e^{-2\pi i\mathbf{Q}^{\perp\!\!\!\perp}\cdot\mathbf{x}^{\perp\!\!\!\perp}} \times W\left[\mathbf{x}^{\perp\!\!\!\perp}-\mathbf{y}^{\perp\!\!\!\perp},\frac{M}{\sqrt{5}}-y_0^{\perp}\right]\right|^2, \quad (41)$$

which obviously reduces to Eq. (39).

To summarize, the intrinsic structure factor for Penrose quasilattices has Bragg peaks at "reciprocal" quasilattice vectors $\mathbf{Q}^{\parallel}$ which can be indexed by five Miller indices[42] $(n_1,n_2,n_3,n_4,n_5)$ according to Eq. (35), and whose intensities are given by Eq. (39) with $\mathbf{Q}^{\perp\!\!\!\perp}$ as in Eq. (36). We show in Fig. 12 the diffraction patterns calculated using Eq. (39) for Penrose quasilattices shown in Fig. 8.

We shall conclude this section by examining the diffraction near a reciprocal quasilattice point. Since $I(\mathbf{Q}^{\parallel})$ is a rapidly varying function of $\mathbf{Q}^{\parallel}$ it is useful to consider some special, simplifying sequences of reciprocal quasilattice points. Thus, we shall analyze $I(\mathbf{Q}^{\parallel}+\mathbf{K}^{m\parallel})$ where $\mathbf{K}^{m\parallel}\to 0$ or $\mathbf{K}^{m\parallel}\to\infty$ as $m\to-\infty$ or $+\infty$, respectively,

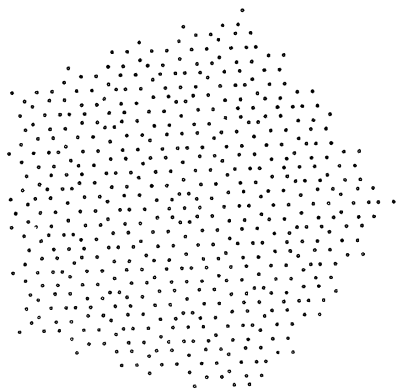

FIG. 11. Extended Penrose quasilattice with $\mathbf{y}^{\parallel}=\mathbf{y}^{\perp\!\!\!\perp}=0$ and $y_0^{\perp}=\sqrt{5}/2$. This tiling is quite different from the one in Fig. 8(d) where $\mathbf{y}^{\parallel}=\mathbf{y}^{\perp\!\!\!\perp}=0$ and $y_0^{\perp}=1/(2\sqrt{5})$. However, since for both tilings $\{y_0\sqrt{5}\}=0.5$ they have identical diffraction patterns (see Fig. 12).

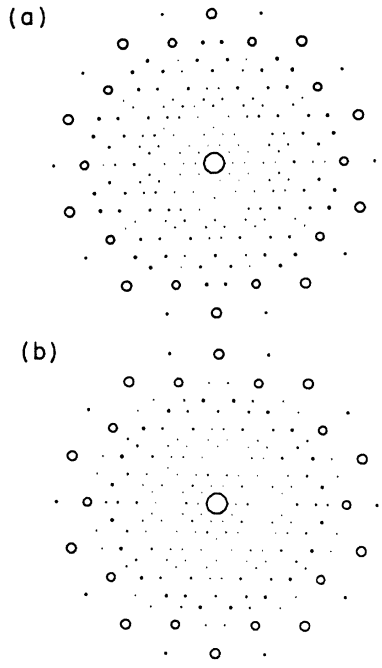


FIG. 12. Diffraction patterns for lattice shown: (a) in Figs 8(a) to 8(c), where $y_0^{\perp}=0$; (b) in Figs. 8(d) to 8(f) and in Fig. 11, where $\{y_0^{\perp}\sqrt{5}\}=0.5$. Note that there is very little difference between the two figures although they represent the maximal possible difference in $\{y_0^{\perp}\sqrt{5}\}$. (Note that by symmetry $\{y_0^{\perp}\sqrt{5}\}$ and $1-\{y_0^{\perp}\sqrt{5}\}$ give identical diffraction patterns.) The fourth ring of diffraction spots from the center corresponds to the fundamental wave vectors and changes very little. The largest change can be seen in the fourteenth ring. The patterns were calculated using Eq. (39) as described in Appendix C. Area of the circles is proportional to the intensity of Bragg peaks at their centers. Only spots with indices $n_i=0,\pm1$ are shown.

following the sequence of reciprocal quasilattice vectors $\mathbf{K}^m$ defined in Appendix B by

$$\mathbf{K}^{m\parallel}\equiv\tau^m\mathbf{K}^{\parallel}\,, \tag{42}$$

$$\mathbf{K}^{m\perp}\equiv(-\tau)^{-m}\mathbf{K}^{\perp}\,, \tag{43}$$

and

$$K_0^{m\perp}\equiv(-2)^m K_0^{\perp}\,, \tag{44}$$

where $\mathbf{K}$ is an arbitrary quasilattice point.

Clearly, in the limit $\mathbf{K}^{m\parallel}\to 0$, Eq. (43) implies $\mathbf{K}^{m\perp}\to\infty$ which in turn implies $W(\mathbf{Q}^{\perp}+\mathbf{K}^{m\perp},\cdot)\to 0$. Therefore, $I(\mathbf{Q}^{\parallel}+\mathbf{K}^{m\parallel})$ will approach zero for every $\mathbf{Q}^{\parallel}$ although $I(\mathbf{Q}^{\parallel})\neq 0$. In other words, this shows that the quasilattice Bragg peaks are indeed isolated. The approach to zero will be governed by the limit of $W(\mathbf{Q}^{\perp}+\mathbf{K}^{m\perp},\cdot)$ as $\mathbf{K}^{m\perp}\to\infty$. For example, for the sharp cutoff $W$ oscillates with a magnitude which decreases as $|\mathbf{K}^{m\perp}|^{-1}\sim|\mathbf{K}^{m\parallel}|$, while for a Gaussian window,[32] $W$ would decrease as $\exp[-\text{const}/|\mathbf{K}^{m\parallel}|^2]$.

In the opposite limit, $\mathbf{K}^{m\parallel}\to\infty$, one has a simple but somewhat surprising result

$$I(\mathbf{Q}^{\parallel}+\mathbf{K}^{m\parallel})\underset{\mathbf{K}^{m\parallel}\to\infty}{\to} I(\mathbf{Q}^{\parallel})\,, \tag{45}$$

where it is assumed that $K_0^{\perp}=0 \bmod\sqrt{5}$.

## V. GEOMETRIC STRUCTURE FACTOR

As mentioned earlier, when a crystal lattice is decorated, the intrinsic structure factor is modified as in Eq. (30). In this section we shall investigate how a decoration of a quasilattice modifies the intrinsic structure factor obtained in preceding section. Since we have seen that a quasilattice can be decorated using two inequivalent methods, we shall have to investigate the two cases separately.

In the first case the quasilattice is decorated by decorating the hyperlattice. This leads to the density given in Eq. (25). This density can be Fourier transformed in the similar manner as the original quasilattice density resulting in

$$\rho^{\parallel}(\mathbf{q}^{\parallel})\sim\sum_{\mathbf{Q}}\delta^{\parallel}(\mathbf{q}^{\parallel}-\mathbf{Q}^{\parallel})e^{-2\pi i\mathbf{Q}^{\perp}\cdot\mathbf{y}^{\perp}}W^*(\mathbf{Q}^{\perp})g(\mathbf{Q})\,, \tag{46}$$

where

$$g(\mathbf{Q})=\sum_{\xi}f_{\xi}e^{2\pi i\mathbf{Q}\cdot\xi}\,. \tag{47}$$

For Fibonacci, icosahedral, or similar quasilattices where there is a one-to-one correspondence between $\mathbf{Q}^{\parallel}$ and $\mathbf{Q}^{\perp}$, Eqs. (46) and (47) lead to the same expression, Eq. (30), for the structure factor as for ordinary crystals, the appropriate geometric structure factor being

$$G(\mathbf{Q}^{\parallel})=|g(\mathbf{Q})|^2=\left|\sum_{\xi}f_{\xi}e^{2\pi i\mathbf{Q}\cdot\xi}\right|^2\,, \tag{48}$$

where $\mathbf{Q}$ is uniquely determined by $\mathbf{Q}^{\parallel}$.

For the case of Penrose quasilattices there is an infinite number of reciprocal vectors $\mathbf{Q}$ associated with a given $\mathbf{Q}^{\parallel}$. Thus, the sums over $\mathbf{Q}$ and $\xi$ mix in Eq. (46). Consequently, the structure factor, Eq. (39), generalizes to

$$S(\mathbf{Q}^{\parallel})\sim\left|\sum_{\xi}f_{\xi}e^{-2\pi i(\mathbf{Q}^{\parallel}\cdot\xi^{\parallel}+\mathbf{Q}^{\perp}\cdot\xi^{\perp})}\sum_{M=0}^{5}e^{i\omega\sum n_j(M-[\xi_0^{\perp}\sqrt{5}])}W\left[\mathbf{Q}^{\perp},\frac{M-\{y_0^{\perp}\sqrt{5}\}+\{\xi_0^{\perp}\sqrt{5}\}}{\sqrt{5}}\right]\right|^2\,, \tag{49}$$

where $[x]$ is the integer part of $x$, i.e., $x=[x]+\{x\}$.

Clearly, when all $\{\xi_0^{\perp}\sqrt{5}\}$ are equal, they just have a role of redefining $\{y_0^{\perp}\sqrt{5}\}\to\{y_0^{\perp}\sqrt{5}\}-\{\xi_0^{\perp}\sqrt{5}\}$ in Eq. (39), and the structure factor simplifies to

$$S(\mathbf{Q}^{\parallel})\sim G(\mathbf{Q})I(\mathbf{Q}^{\parallel},\{y_0^{\perp}\sqrt{5}\}-\{\xi_0^{\perp}\sqrt{5}\})\,, \tag{50}$$

where the geometric structure factor $G$ is defined in Eq. (48) and the intrinsic structure factor $I$, whose explicit $y_0^{\perp}$ dependence is displayed, is defined in Eq. (39).

For a direct decoration of a quasilattice we must start from Eq. (28). This leads to the structure factor

$$S(\mathbf{Q}^{\parallel})\sim\left|\sum_{\mu}g_{\mu}(\mathbf{Q}^{\parallel})i_{\mu}(\mathbf{Q}^{\perp},\{y_0^{\perp}\sqrt{5}\})\right|^2\,, \tag{51}$$

where

$$g_{\mu}(\mathbf{Q}^{\parallel})=\sum_{\xi_{\mu}^{\parallel}}f_{\mu\xi_{\mu}}e^{-2\pi i\mathbf{Q}^{\parallel}\cdot\xi_{\mu}^{\parallel}} \tag{52}$$

and

$$i_{\mu}(\mathbf{Q}^{\perp},\{y_0^{\perp}\sqrt{5}\})=\sum_{M=1}^{5}e^{i\omega M\sum n_j}W_{\mu}\left[\mathbf{Q}^{\perp},\frac{M-\{y_0^{\perp}\sqrt{5}\}}{\sqrt{5}}\right]\,. \tag{53}$$

The two expressions for the structure factor Eqs. (49) and (51) are similar in that the lattice and the decoration contribution mix. The sum over $\mu$ in Eq. (51) is analogous to the sum over $\xi_0^{\perp}$ in Eq. (49). Nevertheless, the two expressions are quite different and it is necessary to elucidate the difference. Therefore, we shall investigate the behavior of the structure factor along the sequence $S(\mathbf{Q}^{\parallel}+\mathbf{K}^{m\parallel})$ defined in Appendix B and in Eqs. (42) to (44) at the end of the preceding section.

As $\mathbf{K}^{m\parallel}\to 0$, we showed that $\mathbf{K}^{m\perp}\to\infty$. Thus, the structure factors, Eqs. (49) and (51) are driven to zero by $W(\mathbf{Q}^{\perp}+\mathbf{K}^{m\perp},\cdot)$ and $W_{\mu}(\mathbf{Q}^{\perp}+\mathbf{K}^{m\perp},\cdot)$, respectively. In the case when $\mathbf{Q}^{\parallel}=\mathbf{Q}^{\perp}=0$, the decoration contribution disappears for Eq. (51) since $g_{\mu}(\mathbf{K}^{m\parallel})\to 1$ and only the quasilattice contribution remains (and approaches zero). However, for Eq. (49) the decoration contribution does not disappear even in this limit. Formally, the

reason is that the term $\xi^{\perp\!\!\!\perp}\cdot\mathbf{K}^{m\,\perp\!\!\!\perp}$ diverges. Physically, this is caused by the fact that the projection of a hyperlattice decoration cannot be in general reduced to a decoration of any finite set of *finite* tiles that is, there is no natural cutoff separating the small wave vector, quasilattice dominated behavior from the large wave vector, decoration dominated one. Accordingly, as $\mathbf{K}^{m\parallel}\to\infty$ the structure factor $S(\mathbf{Q}^{\parallel}+\mathbf{K}^{m\parallel})$ is in both cases dominated by the geometric structure factor as can be easily verified from the fact that $W_\mu(\mathbf{Q}^{\perp\!\!\!\perp}+\mathbf{K}^{m\,\perp\!\!\!\perp},\cdot)$ and $W(\mathbf{Q}^{\perp\!\!\!\perp}+\mathbf{K}^{m\,\perp\!\!\!\perp},\cdot)$ both have well defined limits as $\mathbf{K}^{m\,\perp\!\!\!\perp}\to 0$.

The essential difference between Eq. (49) and Eq. (51) remains even when there is a one-to-one correspondence between $\mathbf{Q}^{\parallel}$ and $\mathbf{Q}^{\perp}$ (like for Fibonacci and icosahedral quasicrystals) in which case one finds

$$S(\mathbf{Q}^{\parallel})=\left|\sum_{\xi} e^{2\pi i\mathbf{Q}\cdot\xi}\right|^2\left|W(\mathbf{Q}^{\perp})\right|^2, \tag{54}$$

and

$$S(\mathbf{Q}^{\parallel})=\left|\sum_{\mu}\sum_{\xi_\mu^{\parallel}} e^{-2\pi i\mathbf{Q}^{\parallel}\cdot\xi_\mu^{\parallel}}W_\mu(\mathbf{Q}^{\perp})\right|^2, \tag{55}$$

respectively.

This difference can be most easily observed in experiments on different quasicrystalline materials which only in the case of Eq. (55) should all have the identical $\mathbf{Q}^{\parallel}\to 0$ diffraction pattern.

## VI. SUMMARY

We have seen that the most general quasicrystal structures based on projected quasilattices can be constructed in two ways: by decorating the tiles of the quasilattice or by decorating the hyperlattice which is projected. An unusual and important feature of quasicrystals in the case of the tile decoration is that, unlike the ordinary crystals, the information about the shapes of the tiles is essential. We demonstrated this in an example.

We calculated the intrinsic structure factor for Penrose quasilattices. For the two methods of decorating a quasilattice we also calculated the total structure factor. In contrast to ordinary crystals, we showed that in general only the hyperlattice-decoration-and-projection method leads to a structure factor which may split into an intrinsic and a geometric factor. For both methods the infinite-wave-vector limit is governed by the decoration. On the other hand, for the tile-decoration method the zero-wave-vector limit depends only on the intrinsic structure factor while for the hyperlattice-decoration-and-projection method the zero-wave-vector limit does not extract the intrinsic structure factor information. The reason is that the latter method of decorating does not lead to a natural definition of a finite number of finite tiles whose size would determine a "boundary" between the intrinsic and the geometric structure factor dominated regions.

Since the icosahedral quasicrystals have been reported in several different compounds, the tile-decoration method could be verified experimentally by finding a universal structure factor behavior near the origin. We pointed out to some characteristic sequences of Bragg spots which are most useful for examining the structure factor. Our specific analysis of pentagonal quasicrystals should especially prove useful in the analysis of the $T$ phase which also occurs in several alloys.

We shall conclude with several remarks. Further elucidation of the effect of tile shapes on the structure factor is necessary. It would be useful to study pentagonal quasilattices which can be obtained as projections from four-dimensional periodic lattices. For such quasilattices the one-to-one relationship between $Q^{\parallel}$ and $Q^{\perp}$ is recovered but an additional complication is created since the *explicit* symmetry is lost.

The effects of thermal fluctuations in quasicrystals are the same as in ordinary crystals—namely they are manifested through the usual Debye-Waller factor $[=\exp(-k_BT\,|\,\mathbf{Q}^{\parallel}\,|^2/3m\omega_0^2)$, in three dimensions at high temperature]. However, different kinds of thermal fluctuations, fluctuations of the window, or of the "atoms," in $\perp$ ("phason") directions probably also occur in quasicrystals. These fluctuations would lead to another factor proportional to $\exp(-c\,|\,\mathbf{Q}^{\perp}\,|^2)$ where $c$ is a function of temperature which depends on whether phasons are annealed or quenched.[43,44] Finally, the finite sample size of a quasicrystal has the same effect as in ordinary crystals, it broadens otherwise sharp Bragg peaks.

Note added. Recently Henley[45] analyzed disk (sphere) packings and local environments in regular two- (three-) dimensional Penrose quasilattices. His Table I agrees with our Table I. Other recent work[46] also analyzes the statistics and decoration of two-dimensional Penrose quasilattices. Its Table I is also in agreement with our Table I.

## ACKNOWLEDGMENTS

I am grateful to the Condensed Matter Theory Group at Harvard for support and hospitality, to D. Nelson for several stimulating discussions and to C. Henley for constructive comments. This work was supported in part by the Petroleum Research Fund administered by the American Chemical Society and by the National Science Foundation through the Harvard Materials Research Laboratory and Grant Nos. DMR 85-14638 and CHE-85-11728.

## APPENDIX A

Following deBruijn[13] we recall that eight different types of vertices occur in regular Penrose quasilattices. They lead to eight Voronoi polygons, two of which are identical in the shape but different in the local environments in which they can be found. They are shown in Fig. 3. DeBruijn also showed that different types of vertices fill disjoint, uniformly and equally dense portions of $U^{\perp}$. The vertices of type $\mu$ fill the sections $U_\mu^{\perp\!\!\!\perp}$ shown in Fig. 9. Therefore, we can immediately determine the frequency of vertices of type $\mu$, which we denote $p_\mu^{\perp\!\!\!\perp}$,

$$p_\mu^{\perp\!\!\!\perp}=\frac{A_\mu^{\perp\!\!\!\perp}}{\sum A_\nu^{\perp\!\!\!\perp}}, \tag{A1}$$

where $A_\mu^{\perp\!\!\!\perp}$ is the area of $U_\mu^{\perp\!\!\!\perp}$, i.e., the area occupied in the perpendicular space by vertices $\mu$. Corresponding fraction

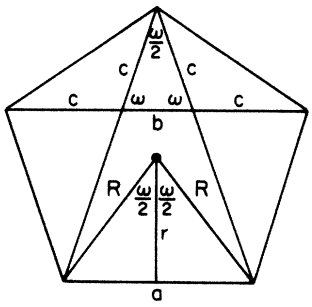


$b=(2-\tau)a$ $\quad A(cbc)=\frac{1}{4}\sqrt{4\tau+3}\,b^2$

$c=(\tau-1)a$ $\quad A(cac)=\frac{1}{4}\sqrt{\tau+2}\,a^2$

$r=\frac{1}{2}\sqrt{\frac{4\tau+3}{5}}\,a$ $\quad A(RaR)=\frac{1}{4}\sqrt{\frac{4\tau+3}{5}}\,a^2$

$R=\sqrt{\frac{\tau+2}{5}}\,a$

FIG. 13. Geometry of a pentagon.

of the area occupied in the $||$ subspace by polygons of type $\mu$ and area $A_\mu^{||}$ is

$$p_\mu^{||}=\frac{A_\mu^{||}A_\mu^{\perp\!\!\!\perp}}{\sum A_\nu^{||}A_\nu^{\perp\!\!\!\perp}}\ . \tag{A2}$$

Formulas (A1) and (A2) are easily evaluated using simple geometric relations shown in Fig. 13 and

$$\cos(2\omega)=-\cos\omega-\frac{1}{2}=-\frac{\tau}{2}\ , \tag{A3}$$

where $\tau=(1+\sqrt{5})/2$ satisfies $\tau^2-\tau-1=0$ and, consequently,

$$\frac{1}{a+b\tau}=\frac{(a+b)}{a^2+ab-b^2}-\frac{b}{a^2+ab-b^2}\tau\ . \tag{A4}$$

The results following from Eqs. (A1) and (A2) are summarized in Table I of the main text.

## APPENDIX B

In this appendix we shall determine certain simple sequences of reciprocal quasilattice vectors $\mathbf{K}^{||}$ whose perpendicular partners $\mathbf{K}^{\perp}$ form equally simple sequences. This is essential for the analysis of structure factors which are functions of $\mathbf{K}^{||}$ implicitly through $\mathbf{K}^{\perp}$ which is a highly irregular function of $\mathbf{K}^{||}$. The simplest approach is to look for a scale change $\mathbf{K}^{||}\rightarrow b\mathbf{K}^{||}$ such that there is a corresponding simple scale change also for the perpendicular component, i.e., $\mathbf{K}^{\perp}\rightarrow c\mathbf{K}^{\perp}$. Formally, we start from *any* $\mathbf{K}$

$$\mathbf{K}=\mathbf{K}^{||}+\mathbf{K}^{\perp}=(P^{||}+P^{\perp})\mathbf{K}\in\mathbf{Z}^D\ , \tag{B1}$$

and we want $b$ and $c$ such that

$$b\,\mathbf{K}^{||}+c\mathbf{K}^{\perp}=(bP^{||}+cP^{\perp})\mathbf{K}\in\mathbf{Z}^D \tag{B2}$$

for every $\mathbf{K}$. That is, $b$ and $c$ must be solutions of Diophantine equations for the components of the matrix $(bP^{||}+cP^{\perp})$,

$$bP^{||}+cP^{\perp}\in GL(D,\mathbf{Z})\ . \tag{B3}$$

For Fibonacci and icosahedral quasilattices one has

$$P^{||}=\frac{1}{5}\begin{bmatrix}2+\tau & 2\tau-1\\ 2\tau-1 & 3-\tau\end{bmatrix} \tag{B4}$$

and

$$P^{||}=\frac{1}{10}\begin{bmatrix}5 & 2\tau-1 & 2\tau-1 & 2\tau-1 & 2\tau-1 & 2\tau-1\\ 2\tau-1 & 5 & 2\tau-1 & 1-2\tau & 1-2\tau & 2\tau-1\\ 2\tau-1 & 2\tau-1 & 5 & 2\tau-1 & 1-2\tau & 1-2\tau\\ 2\tau-1 & 1-2\tau & 2\tau-1 & 5 & 2\tau-1 & 1-2\tau\\ 2\tau-1 & 1-2\tau & 1-2\tau & 2\tau-1 & 5 & 2\tau-1\\ 2\tau-1 & 2\tau-1 & 1-2\tau & 1-2\tau & 2\tau-1 & 5\end{bmatrix}, \tag{B5}$$

respectively (note, $P^{\perp}=1-P^{||}$). This leads to the following solutions of Eq. (B3) (with $D=2$ and 6, respectively):

$$b=\tau,\ \ c=-\tau^{-1}\ , \tag{B6}$$

and

$$b=\tau^3,\ \ c=-\tau^{-3}\ , \tag{B7}$$

respectively. These solutions correspond to $(bP^{||}+cP^{\perp})$ given by

$$\begin{bmatrix}0 & 1\\ 1 & -1\end{bmatrix}, \tag{B8}$$

and

$$\begin{bmatrix}2&1&1&1&1&1\\1&2&1&1&1&1\\1&1&2&1&1&1\\1&1&1&2&1&1\\1&1&1&1&2&1\\1&1&1&1&1&2\end{bmatrix}, \tag{B9}$$

respectively.

In the case of Penrose quasilattices Eq. (B3) has to be slightly generalized to yield

$$bP^{||}+cP^{\perp\!\!\!\perp}+dP_0^{\perp}\in GL(5,\mathbf{Z})\ , \tag{B10}$$

where

$$P^{||}=\frac{1}{5}\begin{bmatrix}2 & \tau-1 & -\tau & -\tau & \tau-1\\ \tau-1 & 2 & \tau-1 & -\tau & -\tau\\ -\tau & \tau-1 & 2 & \tau-1 & -\tau\\ -\tau & -\tau & \tau-1 & 2 & \tau-1\\ \tau-1 & -\tau & -\tau & \tau-1 & 2\end{bmatrix}, \tag{B11}$$

$$P^{\perp\!\!\!\perp}=\frac{1}{5}\begin{bmatrix}2 & -\tau & \tau-1 & \tau-1 & -\tau\\ -\tau & 2 & -\tau & \tau-1 & \tau-1\\ \tau-1 & -\tau & 2 & -\tau & \tau-1\\ \tau-1 & \tau-1 & -\tau & 2 & -\tau\\ -\tau & \tau-1 & \tau-1 & -\tau & 2\end{bmatrix}, \tag{B12}$$

and $P_0^{\perp}=1-P^{||}-P^{\perp\!\!\!\perp}$. A solution of Eq. (B10) is

$$b=\tau,\ \ c=-\tau^{-1},\ \ d=-2\ , \tag{B13}$$

which gives for the left-hand side of Eq. (B10)

$$\begin{bmatrix} 0 & 0 & -1 & -1 & 0 \\ 0 & 0 & 0 & -1 & -1 \\ -1 & 0 & 0 & 0 & -1 \\ -1 & -1 & 0 & 0 & 0 \\ 0 & -1 & -1 & 0 & 0 \end{bmatrix} . \tag{B14}$$

Note that for $\mathbf{K}^{\parallel}$ in some *special* directions different solutions may exist.

## APPENDIX C

We shall explain here how the diffraction patterns in Fig. 12 were calculated. Using Eq. (39) we realize that we need to determine the intersections of $U^{\perp}$ with the planes

$$x_0^{\perp} = \frac{M - \{y_0^{\perp}\sqrt{5}\}}{\sqrt{5}} . \tag{C1}$$

From Fig. 7 we can see that these intersections are the following polygons (projected into the $\perp\!\!\!\perp$ plane).

For $M=1$: regular pentagon with vertices at

$$\mathbf{v}_i^{\perp\!\!\!\perp} \equiv (1 - \{y_0^{\perp}\sqrt{5}\})\mathbf{e}_i^{\perp\!\!\!\perp}, \quad i = 1, \ldots, 5 . \tag{C2}$$

For $M=2$: irregular decagon with vertices at

$$\mathbf{e}_i^{\perp\!\!\!\perp} + \mathbf{v}_{i\pm 3}^{\perp\!\!\!\perp}, \quad i = 1, \ldots, 5 , \tag{C3}$$

For $M=3$: irregular decagon with vertices at

$$\mathbf{e}_i^{\perp\!\!\!\perp} + \mathbf{e}_{i\pm 3}^{\perp\!\!\!\perp} + \mathbf{v}_{i\pm 3}^{\perp\!\!\!\perp}, \quad i = 1, \ldots, 5 . \tag{C4}$$

For $M=4$: irregular decagon with vertices at

$$-\mathbf{e}_i^{\perp\!\!\!\perp} - \mathbf{e}_{i\pm 3}^{\perp\!\!\!\perp} + \mathbf{v}_{i\pm 3}^{\perp\!\!\!\perp}, \quad i = 1, \ldots, 5 . \tag{C5}$$

For $M=5$: regular pentagon with vertices at

$$-\mathbf{e}_i^{\perp\!\!\!\perp} + \mathbf{v}_i^{\perp\!\!\!\perp}, \quad i = 1, \ldots, 5 . \tag{C6}$$

In all of these equations the indices should be taken mod5.

The Fourier transforms of these polygons, which enters Eq. (39), can be evaluated by breaking up the polygons into triangular sections and using the formula

$$F(\mathbf{q};\mathbf{a}_1,\mathbf{a}_2) \equiv \int_{\Delta(\mathbf{a}_1,\mathbf{a}_2)} d^2\mathbf{x} e^{2\pi i \mathbf{q}\cdot\mathbf{x}}$$
$$= -\frac{1}{(2\pi)^2} \frac{\det(\mathbf{a}_1\mathbf{a}_2)}{\mathbf{a}_1\cdot\mathbf{q}\mathbf{q}\cdot\mathbf{a}_2}$$
$$\times \left[ \frac{\mathbf{q}\cdot(\mathbf{a}_2 e^{2\pi i \mathbf{q}\cdot\mathbf{a}_1} - \mathbf{a}_1 e^{2\pi i \mathbf{q}\cdot\mathbf{a}_2})}{\mathbf{q}\cdot(\mathbf{a}_1 - \mathbf{a}_2)} + 1 \right] \tag{C7}$$

for the two-dimensional Fourier transform of the triangle formed by $\mathbf{a}_1$ and $\mathbf{a}_2$ radiating from the origin.


*On leave from: Department of Physics, North Dakota State University, Fargo, ND 58105; Address after September 1, 1986: Center for Theoretical Physics, Texas A & M University, College Station, TX 77843.

[1]D. Shechtman, I. Blech, D. Gratias, and J. W. Cahn, Phys. Rev. Lett. **53**, 1951 (1984); P. A. Bancel *et al.*, *ibid.* **54**, 2422 (1985); S. J. Poon *et al.*, *ibid.* **55**, 2324 (1985).

[2]A. L. Mackay, Kristallografiya **26**, 910 (1981) [Sov. Phys.—Crystallogr. **26**, 517 (1981)].

[3]A. L. Mackay, Physica (Amsterdam) **114A**, 609 (1982).

[4]D. Levine and P. J. Steinhardt, Phys. Rev. Lett. **53**, 2477 (1984).

[5]P. A. Kalugin, A. Yu. Kitaev, and L. S. Levitov, Pis'ma Zh. Eksp. Teor. Fiz. **41**, 119 (1985) [JETP Lett. **41**, 145 (1985)]; J. Phys. Lett. (Paris) **46**, 601 (1985).

[6]P. Bak, Phys. Rev. Lett. **54**, 1517 (1985); Phys. Rev. B **32**, 5764 (1985); in *Scaling Phenomena in Disordered Systems*, edited by R. Pynn and A. Skjeltrop (Plenum, New York, 1985).

[7]V. Elser, Phys. Rev. B **32**, 4892 (1985); Acta Crystallogr. Sect. A **42**, 36 (1986).

[8]R. K. P. Zia and W. J. Dallas, J. Phys. A **18**, 341 (1985).

[9]M. Duneau and A. Katz, Phys. Rev. Lett. **54**, 2688 (1985); A. Katz and M. Duneau, J. Phys. (Paris) **47**, 181 (1986).

[10]P. Kramer (unpublished).

[11]F. Gähler and J. Rhyner, J. Phys. A **19**, 267 (1986).

[12]By "quasilattice" we shall mean an aperiodic array of isolated *identical* points (point scatterers) whose Fourier transform consists of sharp Bragg peaks. This is not meant as a rigorous definition, it only serves to stimulate certain intuition.

[13]N. G. deBruijn, Ned. Akad. Weten. Proc. Ser. A **43**, 39 (1981); **43**, 53 (1981).

[14]P. Kramer and R. Neri, Acta Crystallogr. Sect. A **40**, 580 (1984).

[15]P. M. de Wolff, Acta Crystallogr. Sect. A **30**, 777 (1974).

[16]A. Janner and T. Janssen, Phys. Rev. B **15**, 643 (1977); Physica (Amsterdam) **99A**, 47 (1979); T. Janssen (unpublished).

[17]P. Bak, Phys. Rev. Lett. **56**, 861 (1986).

[18]J. E. S. Socolar, P. J. Steinhardt, and D. Levine Phys. Rev. B **32**, 5547 (1985); D. Levine and P. J. Steinhardt, *ibid.* **34**, 596 (1986).

[19]This discovery is sometimes attributed to R. Ammann (see Ref. 4). From Ref. 2 alone it is not clear whether R. Ammann is credited for discovering the icosahedral tiling or the packing of the two unit cells into the rhombic triacontahedron.

[20]A more complete description in terms of certain matching rules is given by J. E. S. Socolar and P. J. Steinhardt, Phys. Rev. B **34**, 617 (1986).

[21]Different icosahedral *central* tilings whose Fourier transform is not well understood were discussed by P. Kramer [Acta Crystallogr. Sect. A **38**, 257 (1982)] and R. Mosseri and J. F. Sadoc [in *The Structure of Non-Crystalline Materials*, edited by P. H. Gaskell, J. M. Parker, and E. A. Davis (Taylor and Francis, London, 1982)].

[22]S. Ostlund and R. Pandit, Phys. Rev. B **29**, 1394 (1984).

[23]J. P. Lu, T. Odagaki, and J. L. Birman, Phys. Rev. B **33**, 4809 (1986).

[24]F. Nori and J. P. Rodriguez, Phys. Rev. B (to be published).

[25]See, for example, M. Gardner, Sci. Am. **236**, 110 (1977).

[26]R. Penrose, Bull. Inst. Math. Appl. **10**, 216 (1974).

[27]By Penrose quasilattice we mean the set of vertices of a Penrose tiling.

[28]L. Bendersky, Phys. Rev. Lett. **55**, 1461 (1985); L. Bendersky *et al.*, Scripta Metall. **19**, 909 (1985).

[29]We recall that for a set of points $\mathbf{x}_j$, $j=1, \ldots,$ Voronoi polygon at $\mathbf{x}_i$ can be specified in terms of polar coordinates at

$\mathbf{x}_i$ by the equation

$$r=\frac{1}{2}\min_j\left[\frac{|\mathbf{x}_j-\mathbf{x}_i|^2}{\hat{\mathbf{n}}\cdot(\mathbf{x}_j-\mathbf{x}_i)}\right],\quad \hat{\mathbf{n}}(x_j-x_i)>0\ ,$$

where $r\hat{\mathbf{n}}\equiv\mathbf{x}-\mathbf{x}_i$.

[30]Note that the same type of Voronoi polygon, a pentagon, is associated with two different types of vertices. We will consider these two pentagons as distinct since they have distinct varieties of next nearest local environments. Also note that each polygon appears in all orientations generated by the tenfold symmetry.

[31]Hereafter we shall call a periodic lattice simply a lattice.

[32]For example, S. Sachdev and D. R. Nelson [Phys. Rev. **32**, 4592 (1985)] take $\rho$ to be a set of Gaussians located at the hyperlattice points and they take a cut to obtain a quasilattice density. Equivalently, their choice could be interpreted as that of a Gaussian window and the usual density Eq. (1).

[33]We assume the lattice parameter equal to unity. For arbitrary lattice parameter $l$ all quantities which we write would have to be multiplied by a power of $l$ dictated by the dimension of the quantity.

[34]Note, however, that two quasilattices with different $\mathbf{y}^{\perp}$ and $\mathbf{y}^{\parallel}=0$ might be only translations of each other.

[35]Quasilattices with $y_0^{\perp}\neq 0$ we shall call *extended* Penrose quasilattices. Two quasilattices with different $y_0^{\perp}$ (mod$1/\sqrt{5}$) fall into different local isomorphism classes. The concept of local isomorphism classes is discussed in Ref. 18.

[36]The variation in the density of singular Penrose tiles relative to the regular tiles does not occur if $U$ is taken to be a single vertex plus its *open* hypercube. We always assume $U$ to be a *closed* unit hypercube.

[37]As mentioned earlier in the text (see Ref. 17), a quasicrystalline structure can be always represented as a cut through a hypercrystalline structure. From this point of view the concept of a quasilattice and of its decoration is not very helpful. However, determination of atomic positions in a quasicrystal requires determination of atomic *surfaces* in the hypercrystal. Since nothing is known about the chemistry of such surfaces, this approach to structure determination is not very promising at the present time.

[38]In practice, one would like to know how to determine the structure of a quasicrystal from its diffraction pattern. In this paper we want to understand how to determine the diffraction pattern associated with a given structure.

[39]J. Peyrière, J. Phys. (Paris) Colloq. **47**, C3-41 (1986).

[40]This is a concrete expression of the conclusion of Ref. 18 that two tilings in the same local isomorphism class (same $y_0^{\perp}$) have identical diffraction patterns, whereas tilings in different local isomorphism classes (different $y_0^{\perp}$) have distinct diffraction patterns.

[41]By going to the continuum one generates a factor proportional to the number of quasilattice points, just as one would expect because of the $\delta$ functions in Eq. (32).

[42]Since $(n_1,n_2,n_3,n_4,n_5)$ can be specified only mod(1,1,1,1,1), four (infinite-range) indices would suffice. For symmetry reasons it is more convenient to keep five indices.

[43]M. V. Jarić, in Internationl Workshop in Aperiodic Crystals, edited by D. Gratias and L. Michel [J. Phys. (Paris) Colloq. **47**, C3-259 (1986)]; M. V. Jarić, D. R. Nelson, and U. Mohanty (unpublished).

[44]V. Elser, Phys. Rev. Lett. **54**, 1730 (1985); if the idea of the unit tiles is to be taken seriously, then there is no reason to assume that the tiles would be Penrose rhombuses and not some other congruently deformed tiles, which would then exclude the possibility for scrambling of the tiles considered by Elser.

[45]C. L. Henley, Phys. Rev. B **34**, 797 (1986).

[46]V. Kumar, D. Sahoo, and G. Athithan (unpublished).